Expert Systems with Applications 40 (2013) 7534–7543

Contents lists available at ScienceDirect

Expert Systems with Applications

journal homepage: www.elsevier.com/locate/eswa

A mass classification using spatial diversity approaches in mammography images for false positive reduction

Geraldo Braz Junior [a,*], Simara Vieira da Rocha [a], Marcelo Gattass [b], Aristófanes Corrêa Silva [a], Anselmo Cardoso de Paiva [a]

[a] Federal University of Maranhão, Applied Computing Group – NCA, Av. dos Portugueses, 1996, Campus do Bacanga, São Luis, Maranhão 65080-805, Brazil
[b] Catholic University of Rio de Janeiro, Tecgraf – Group of Computer Graphics Technology, Rua Marquês de São Vicente 225, Rio de Janeiro 22453-900, Brazil

ARTICLE INFO

Keywords:
Mammography
Pattern recognition
False positive reduction
Spatial diversity analysis

ABSTRACT

Breast cancer is configured as a public health problem that affects mainly women population. One of the main ways of prevention is through screening mammography. The interpretation made by the physician is a repetitive task because of a low contrast image and the examination of several exams. So, computer systems have been proposed to aid detection step and helps physician, with the aim to increase sensitivity at the same time that reduces invasive procedures. Although these systems had improved the sensitivity of the original examination of mammography, they also generate a lot of false positives. This paper presents a methodology for reducing false positives by analyzing the diversity of approaches with improved spatial decomposition. After experiments the results reaches a high level of sensitivity at the same time promote a high rate of reduction of false positives.

1. Introduction

According to the estimation of the American Cancer Society, the chance of a woman having the breast cancer sometime during her life is about 1 in 8, and the chances of dying from the disease is of 1 in 35 (ACS, 2011). The screening mammography is the best way for the precocious detection of any kind of lesion in breast, also cancers. An earlier diagnosis improve the chances of cure.

It is also know that in early stages, the treatment is more effective. The digitized mammogram is a image that presents overlapping breast tissues obtained by the X-ray exposure. The overlap and physiological characteristics of the patient can generate a mammogram of low contrast which could lead the physician a wrong diagnostic caused by the repetitive task of analyzing the zimage (Karssemeijer, Frieling, & Hendriks, 1993).

Efforts has been made in the use of image processing and pattern recognition techniques to improve the breast cancer diagnosis results. The goal is to increase detection and diagnostic accuracy providing a second opinion also causing a reduction in the rate of false positive biopsies for cases since the sensitivity of mammography exam is around 85% (Houssami, Ciatto, Irwig, Simpson, & Macaskill, 2002).

The main objective of the Computer Aided Detection Systems (CAD) is to provide a second opinion and a more efficient detection. This is characterized by a high rate of sensitivity at the same time a small number of false positive regions considered to be generated. These systems have improved the sensitivity or detection rate of lesions (Dean & Ilvento, 2006; Freer & Ulissey, 2001; Ko, Nicholas, Mendel, & Slanetz, 2006). Some surveys revise promising work in the area are (Bozek, Mustra, Delac, & Grgic, 2009; Cheng et al., 2006; Elter & Horsch, 2009; Nanni, Lumini, & Brahnam, 2012; Tang, Rangayyan, Xu, El Naqa, & Yang, 2009).

However, these systems have been tested on actual studies and has generated many false positives causing an increase of the biopsy rate in some situations (Burhenne et al., 2000; Fenton et al., 2007; Rangayyan, Ayres, & Desautels, 2007). The problem of reducing false positives is challenging for the area of computer vision and pattern recognition. The improvement of their performance is essential for the generation of more efficient systems with real potential to help physician in their task of interpreting mammograms.

Several approaches uses features based on texture (Eltoukhy, Faye, & Samir, 2010a; Lladó, Oliver, Freixenet, Martí, & Martí, 2009; Moayedi, Azimifar, Boostani, & Katebi, 2010), or by the cumulative distribution information of the texture (Braz Junior, Paiva, Silva, & Oliveira, 2009; Carvalho, Paiva, & Silva, 2012; Hussain, Khan, Muhammad, & Bebis, 2012; Masotti, Lanconelli, & Campanini, 2009; Eltoukhy, Faye, & Samir, 2010b), geometry or shape (roundness, sphericity, spicularity) (Tralic, Bozek, & Grgic, 2011) (Cheikhrouhou, Djemal, & Maaref, 2011; Surendiran & Vadivel,

* Corresponding author. Tel.: +55 9888425303.
E-mail addresses: geraldo@deinf.ufma.br (G. Braz Junior), simara@deinf.ufma.br (S.V. da Rocha), mgattass@tecgraf.puc-rio.br (M. Gattass), ari@nca.ufma.br (A.C. Silva), paiva@deinf.ufma.br (Anselmo Cardoso de Paiva).

0957-4174/$ - see front matter © 2013 Elsevier Ltd. All rights reserved.
http://dx.doi.org/10.1016/j.eswa.2013.07.034

2010; Varela, Timp, & Karssemeijer, 2006), morphological or nominal (BI-RADS information or patient's medical history) (Liu, Liu, Zhou, & Tang, 2010; Shi et al., 2008; Verma, 2008).

We have verified that the false positive reduction of the regions extracted from the mammogram as mass and non-mass is a crucial stage in the methodologies for detection of breast cancer and that there is a potential to be explored in measurements that describe texture as the diversity indexes applied analyzed in a directional approach. This study began in previous work of the group (Braz Junior, Rocha, Silva, & Paiva, 2013; Sampaio, Diniz, Silva, Paiva, & Gattass, 2011; Carvalho, Paiva, & Silva, 2012; Nunes, Silva, & Paiva, 2010), which demonstrate the effectiveness of these methods.

This work proposes the use of spatial approach of diversity indexes (Shannon-Wiener, McIntosh, Total Diversity, Brillouin, Simpson, Berger-Parker, J, ED, Hill, Buzas-Gibson, Camargo) to describe the patterns found in previously segmented regions of mammogram. We use Support Vector Machines to recognize the generated feature vector and classify the regions into mass or non-mass classes. The main goal is to propose an efficient false positives reduction methodology and assist detection approach to helps the physician on the task of searching and identifying breast cancer. The contribution of this study is to measure the impact of the spatial analysis of ROI's subregions and describe small local variations with diversity analysis that helps in the description of this standard.

The remainder of this work is organized as follows. Section 2 brings a brief introduction to Diversity Indexes. Section 3 presents a detailed description of the proposed methodology and evaluation used in this work. Section 4 presents and discusses about the founded results. Finally, Section 5 presents the final considerations.

2. Diversity analysis

The proposed methodology in this work is inspired in biological process using diversity analysis. Following we present the Diversity Indexes used as texture feature descriptors as well as the mapping of this problem to a traditional image processing task.

The Diversity Analysis intends to identify the distribution of a group of species and their interrelations. It is used in Ecology to measure the biodiversity in an ecosystem. The diversity refers to the variety of species in a given community or habitat. Biodiversity is the relationship between the number of species (richness), the pattern of distribution of individuals in their species (evenness) and the dominance of one or more species among others (dominance). All these characteristics can be measured and investigated using indexes usually classified as coverage of local analysis (alpha) or between various habitats (beta) (Magurran, 2004).

More generally, the diversity indexes can be used to measure the diversity of a population where each member belongs to one single group or specie. This paper intends to study the use of Diversity indexes for false positive reduction in pattern recognition process to distinguish mass and non-mass ROI's extracted from a digitized mammography image. With this goal we adopt that the pixels are the individuals and their tonalities represents the set of species.

Considering that each image ROI used has a distribution of gray tones varying from 0 to 255 (8 bits per pixel). Any pixel x of image A have a specie s_i. The set given by $x_0,x_1,\ldots,x_N$ represents the overall population P where N is the total number of individuals and also of pixels. The set S is the total amount of species of the set $s_0,s_1,\ldots,s_i$ where i represents a specific specie. The number of individuals of each species is represented by n_i, and p_i is the total proportion of the sample belonging to species i, that is $p_i = \frac{n_i}{N}$. With these definitions started (the following equations are based on them), this paper investigates the application of the following diversity indexes for texture characterization of mammogram images.

The Shannon-Wiener's Index (H) is derived from the Information Theory. It shows the degree of uncertainty that exists from one specie over his community (Shannon, 2001). The calculation is defined by:

$$H = -\sum_{i=1}^{S} p_i \ln p_i \tag{1}$$

It is not necessary to know *a priori* the entire population distribution and species to use the index. Rare and abundant species have equal weights in Shannon-Wiener's. Bigger values of the index represent bigger heterogeneity of the population under study, so bigger richness. Also, similar values taken from separate populations represent evenness over all species.

Using the McIntosh Index (Mc) (Magurran, 1988) a population can be seen as a point in an S-dimensional hyper-volume and the Euclidean distance from the community to the origin can be used as a diversity measurement, defined by:

$$Mc = \frac{N - U}{N - \sqrt{N}} \tag{2}$$

where $U = \sqrt{\sum_{i=1}^{S} n_i}$ is a Euclidean distance from the origin to the population. The value of the index varies from 0, if there is just one specie, to 1, if the diversity is maximum (each individual is of a different specie).

The Total Diversity Index (Td) (Magurran, 1988) estimates the total richness of a population based on species variation. This measure is given by:

$$Td = \sum_{i=1}^{S} w_i(p_i(1 - p_i)) \tag{3}$$

where w_i is the weight or importance given individually to a specie characterized by $\frac{1}{n_i}$.

The Brillouin Index (Hb) (Pielou, 1975) measures the richness of a known population and it is recommended when that population is not random. Also, this index tends to inform similar results comparable to Shannon-Wienner's Index (Shannon, 2001) used in a not completely known population. It is defined by:

$$Hb = \left(\frac{1}{N}\right)(\log N! - \sum_{i=1}^{S} \log n_i!) \tag{4}$$

The Simpson Index (Ds) is a second order statistical feature that informs the probability of two randomly individuals selected from a community to belong to the same specie (Simpson, 1994). Its main use is to summarize the representation of this diversity in a single value capable of qualifying this region as very heterogeneous or uniform.

$$Ds = \frac{\sum_{i=1}^{S} n_i(n_i - 1)}{N(N - 1)} \tag{5}$$

Like Shannon's Index, Simpson's Index takes into account the richness of the species and is a measurement of the relative abundance of each species (Hill, 1973). The values obtained for the Simpson's Index are in the interval from 0 to 1, where the value 0 represents infinite diversity in the sample and 1 means that there's no diversity.

The Berger-Parker Index (Bp) (May, 1975) is the numerical importance of the most abundant species, defined by:

$$Bp = \frac{max(n_i)}{N} \tag{6}$$

where $max(n_i)$ is the amount of the most abundant specie.

The J Index (J) (Pielou, 1975) compares the observed Shannon-Wiener Index against the distribution of individuals between the observed species which would maximize diversity, and is defined by:

$$J = \frac{H}{H'} \tag{7}$$

where $H$is the Shannon-Wiener Index calculated by $H = -\sum_{i=1}^{S} p_i \ln p_i$ and his maximum value H' is given by $H' = logS$.

The ED (Ed) (Magurran, 1988) Index compares the dominance of Simpson with the known species that maximize the diversity. It is a relation between Simpson index $D$and it's maximum:

$$Ed = \frac{Ds}{Ds'} \tag{8}$$

where $Ds$is the Simpson Index (Simpson, 1994) given by $Ds = \frac{\sum_{i=1}^{S} n_i(n_i-1)}{N(N-1)}$ and his maximum dominance Ds' calculated by $Ds' = \left(\frac{S-1}{S}\right) * \left(\frac{N}{N-1}\right)$.

The Hill Index (Hill) (Jost, 2010) calculates the equally abundance distribution of the species, given by:

$$Hill = \frac{\frac{1}{Ds-1}}{e^H - 1} \tag{9}$$

where $Ds$and $H$are respectively the Simpson and Shannon-Wienner's Indexes previously explained. In this index, if the species are equally abundant then the index should take the maximum value. This value will decrease as the relative abundance differ between species.

The Buzas-Gibson Index (Bg) (Buzas & Hayek, 1998) indicates the degree of evenness trough Shannon index $H$and is defined by:

$$Bg = \frac{e^H}{S} \tag{10}$$

where H is given by Shannon-Wienner's Index.

The Camargo Index (E) (Camargo, 1993) it is a evenness index that do not considerate species richness, thus it is not affected by rare species on the population. It takes into account the relative proportion of a certain species compared to all other species and is defined by:

$$E = 1 - \left(\sum_{i=1}^{S}\sum_{j=i+1}^{S} \frac{p_i - p_j}{S}\right) \tag{11}$$

3. Proposed Methodology

Detection methodologies generates a large number of false positives that could cause mistakes for the physician interpretation. So one of the main problems to be solved on this kind of methodology is how to generate responses as faithfully as possible to permit assist correctly the physician on the task of the interpretation of the exam. The proposed methodology is organized into five steps, exemplified in Fig. 1 that is acquisition of the mammogram regions (ROI); enhancement of these regions through logarithm transformation and multilevel decomposition; feature characterization using Spatial diversity analysis and classification of the original regions into mass or non-mass using Support Vector Machines. Finally the validation of the results. The following section will explain the methodology steps.

3.1. Acquisition

The first step of this study is to obtain regions of interest (ROI) extracted from digitized mammograms. We used ROI's extracted from the DDSM – Digital Database for Screening Mammography (Heath, Bowyer, & Kopans, 1998).

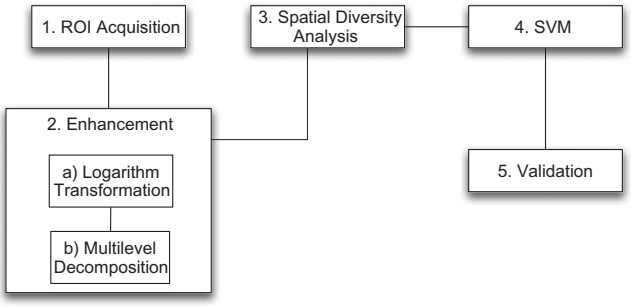

Fig. 1. Steps of the Proposed Methodology for mass classification.

The DDSM mammogram database has cases acquired in 2620 through the following American institutions: Massachusetts General Hospital, Wake Forest University, and Washington University in St. Louis School of Medicine. The data consist of studies of patients of different ethnic and racial groups. Each case contains two pictures of each breast, the projections mediolateral oblique and craniocaudal, thus consisting of four mammography images. The database also provides information regarding the patient, such as age and density of the breast. Are also informed the type of scanner used and the resolution of each image.

Images that have suspicious areas, presents a text describing the abnormality diagnosis and the location thereof. The descriptions of lesions in the mammograms follow the terms published in the lexicographical BI-RADS. These clinical findings were previously targeted by computational methods and in a next step, enhanced by experts. The images have a resolution and color depth different. For standardization of the following algorithms, the images were transformed to 8 bits per pixel before extracting regions of interest.

Were extracted a total of 1600 regions of interest. Compound of 400 mass (200 benign and 200 malignant) and 1200 non-mass regions. The mass regions were obtained accordingly to the information provided by DDSM that refer to location, contour and type of abnormality. The non-mass regions were obtained automatically from the same mammograms that were extracted the mass regions. The regions does not share similar area with anomalies, pectoral muscle or image background and corresponds only breast to parenchyma.

The proportion of non-mass regions is three times greater to simulate a detection process, where it usually generates a large number of false positives compared to the number of true positives.

3.2. Logarithm and multilevel enhancement

The DDSM ROI's are initially subjected to a process of enhancement. This step aim to increase the distinction of textures representing masses. The enhancement is accomplished in two steps.

The first is the application of the logarithm transformation. The purpose of this filter is to enhance the participation of grayscale with few occurrence in the overall distribution of the image. Fig. 2 gives an example of applying the logarithmic transformation for a mass ROI.

The second step consists in decomposing the image into six other range images with different maximum values. We call this as multilevel decomposition. The purpose is to generate various quantizations, calculated linearly, of the same image and helps to coding grayscale standards presents in different clusters. Are used as tracks (2^8, 2^7, 2^6, 2^5, 2^4 and 2^3).

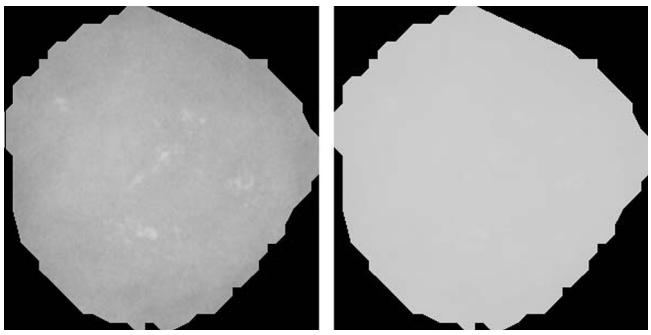

Fig. 2. Logarithmic enhancement applied for a mass ROI. At left, the original ROI. At right, after enhancement.

3.3. Spatial diversity texture analysis

Each sample generated after the enhancement step was submitted to a spatial texture analysis using the Diversity Indexes presented in Section 2. The spatial analysis measures the autocorrelation between the points over a certain localization, distance and direction. Our goal is to measure also the autocorrelation information besides their diversity and use this information to detect patterns.

Fig. 3 presents the steps to perform the spatial diversity texture analysis. We initially perform a spatial decomposition of the region of interest using different strategies. These divisions preserve spatial neighborhood associations and concentration of the species into each one. Our goal is to codify the species distribution over each subregion and enhance the spatial agglomeration of certain specie over all population.

The original region is decomposed into subregions under three approaches: VHD that divide the region in Horizontal, Vertical, or Diagonal windows, Circular (CIRC), Ring (RING).

The VHD approach creates non-overlapping zones to measure the influence of the heterogeneity in scattered locations in the diversity analysis. It is done using four specific decomposition, where each represents a division of the original ROI. These subdivision are:

- Horizontal: the ROIS's are subdivided into horizontal strips with equal area (Fig. 4(a)).
- Vertical: the ROI's are subdivided into vertical strips with equal area (Fig. 4(b))
- Window: Vertical and Horizontal junction, causing the division of the region in the same area windows (Fig. 4(c))
- Centralized Window: also Vertical and Horizontal junction, but generating a central window over a bigger area then the edge windows, as exemplified in Fig. 4(d)
- Diagonal: the division of the region into triangles following the separation of main and secondary diagonals (Fig. 5)

The amount of horizontal and vertical strips are configurable. Also the amount of windows. The central window corresponds to 50% of the total area of the entire ROI for centralized window decomposition. Also, this decomposition generates other eight

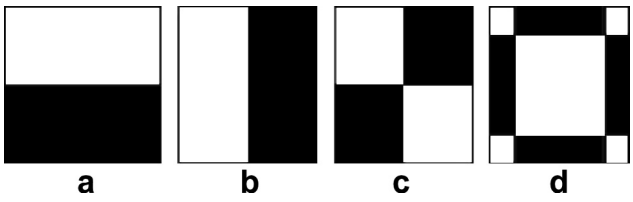

Fig. 4. Rectangular decomposition's applied in the ROI to preserve local associations before applying methods of description. In (a) Horizontal (b) Vertical, (c) Windows, (d) Centralized Windows.

edge subregions. The diagonal decomposition always generates four subregions.

The Circular approach subdivide the ROI in concentric circular regions. The aim is to analyze the growth of the distinction of concentric regions considering that a mass has a core region more homogeneous than a non-mass region. An example of this decomposition is represented in Fig. 6.

The radius of each circle is computed based on the maximum radius. The maximum radius is computed as the half of the lowest dimension (width or height). To obtain each radius used by circular approach, we use the following equation:

$$R_i = \frac{R_{max}}{i} \tag{12}$$

where $i = 1,2,3 \ldots ,n$ and n is the amount of circles chosen by the methodology.

The Rings approach follows the same principle of Circular approach and it is exemplified by Fig. 7. The basic difference lies in the fact of how it comes to rings. Two consecutive circle share same center, so a ring is the area represented by the difference between then. Thus, the radius of the inner ring is used as a minimum radius to the next.

From the same calculation of the maximum radius obtained by the decomposition of circles, the following equation obtain the area delimited by the ring:

$$Ring_i = C_i - C_{i-1} \tag{13}$$

where $i = 2,3,3 \ldots (n+1)$ and $n+1$ is the amount of rings chosen by the methodology, function C represents the area of a circle with radius i obtained proportionally using the relation used to obtains circles.

Each decomposition generates subregions that will go through the process of description of Diversity analysis. The diversity indexes used are: Shannon-Wiener, Simpson, J, Ed, Buzas-Gibson, Camargo, Hill, McIntosh, Total Diversity, Brillouin, Berger-Parker.

By applying these indexes, we extract a measurement of the diversity for each subregion generated by the decomposition approach. As the index computes a global evaluation of the community diversity, it may not capture some information of rare species. In order to capture this we propose that the methodology divides the species into subpopulations (small communities).

The division is made by non-linear quantization. It was verified that a region may or may not contain all the possible species. Also is know that these species are not necessarily grouped in a certain range of values. Therefore, the procedure performed to capture

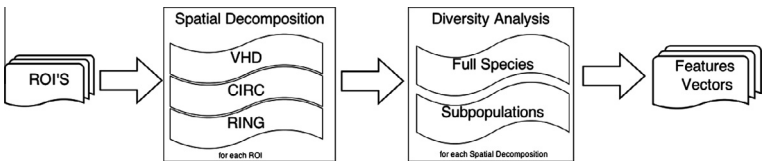

Fig. 3. Steps of spatial diversity texture analysis.

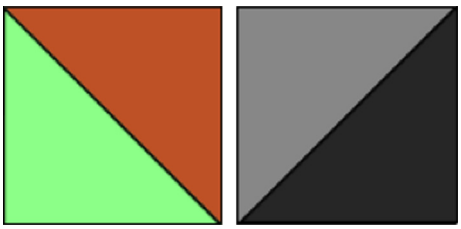

Fig. 5. Representation of the decomposition in diagonal.

these subpopulations is obtained dividing then in equal amounts of subpopulations, from a ordered gray tonality list of species. The number of species in each population subgroup is always constant. We named this restriction as DIV.

3.4. Pattern recognition using support vector machines

The set of spatial diversity features generated for each sample was classified using Support Vector Machine (SVM) (Vapnik, 2000). SVM is a machine learning technique based on the creation of a high dimensional hyperplane of separation optimizing the limits of generalization.

SVM's was previously used for breast tissues classification (Braz Junior et al., 2009; Sampaio et al., 2011; Carvalho et al., 2012; Hussain et al., 2012), with success and has been demonstrating over the literature to provide high performance, mainly in the capacity of generating learning generic models. For the proposed methodology, we also use SVM because it makes easy to adjust the learning model. In addition, the generated model consists of feature vectors of the training base, called support vectors. This make easy to analyze the generalization capability of the extracted features, given regarding the number of support vectors used to create the model. As lower is this number, better is the ability of generalization. In SVM's that number is also directly connected to the test accuracy. In the case of a overfit, which is characterized by the large number of support vectors, usually the test accuracy is low because of the low ability of generalization.

To lead with different data distribution, it is allowed to map the features space to another high dimension space where it is possible to creation a hyperplane of discrimination. Here we use Radial kernel to map the characteristics. This kernel is defined as:

$$K(x,y) = e^{-\gamma\|x-y\|^2} \tag{14}$$

where $\gamma > 0$ is a parameter that also is defined by the user.

SVM has the penalty parameter C that regulates the classification function for the best overall accuracy. This parameter was calculated for each set of samples during the training stage as the parameter $\gamma$for radial function. Also, aiming to give more importance classification to the mass class, we adjusted the weight penalty imposed on the mass group. This parameter will allow the SVM to prioritize Sensibility even if there is no balancing between classes.

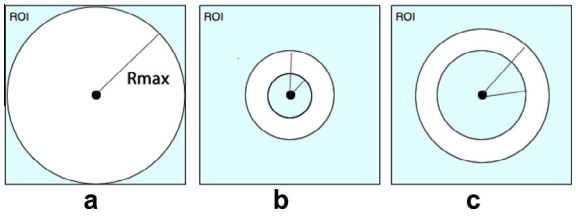

Fig. 7. Representation of Rings decomposition. The ring is represented in b and c as the difference between the inner circle and one outer circle.

The classification process starts with a definition of a set of training samples and test samples, always in a random way. We use two proportion for the division, that is 50/50 and 60/40 to reflects a normal situation where the training and testing base has almost the same number of individuals. The first one, use half base for training and the other one uses 60% of the samples for training. In order to avoid biased results, it was made three random sets for each configuration. The final result is presented in terms of the average result jointly with the standard deviation.

3.5. Validation

The result of the recognition step is the identification of the ROI as mass or non-mass. The mass class is the positive one and is called as true positive. The non-mass ROI's are called true negative. When a ROI of mass class is considered a non-mass ROI we name it as false negatives. On the other hand, when a non-mass ROI is classified as mass we named as false positive.

The clinical value of a test is related to its specificity and sensitivity (Altman & Bland, 1994). It should provide a good preliminary indication of which individuals have the disease and which do not, and this can only be achieved if the methods used are valid.

The sensitivity (S) is the mass proportion of subjects who have a positive test, i.e. the probability of being mass, an individual having a positive test (percentage of times that the test hits). Specificity (Sp) is the non-mass proportion of individuals not having a negative test or the likelihood of not being unusual, having a negative test. The sensitivity is defined, therefore, as the ability of a test to properly identify those individuals who have a certain mass, while the specificity is defined as the ability of the test to correctly identify those that do not.

In addition to the sensitivity and specificity, the overall Accuracy (Acc) is used as the parameter, and the extent of generalization of the model inferred from the number of support vectors used in the classification.

4. Experiments and results

The experiments were conducted according to the presented methodology in Section 3. The parameters used for spatial decomposition was four divisions for horizontal, vertical and diagonal subdivision, nine windows (for windows and centralized window) and also five radius for Rings and Circular decomposition. For all

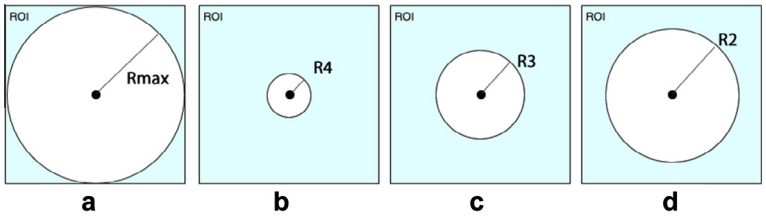

Fig. 6. Circular approach. All circles shares equal center but have increase radius, where the maximum radius is represented by (a). As the radius increases, different portions of the ROI are capture as exemplified inf b–d.

texture description was used a division of one (global) or four (DIV) species division to make subpopulations.

The parameters of the SVM are estimated for each configuration (spatial approach, diversity index, proportion), and the weight parameter for the class mass is always set to 3, corresponding to the base degree unbalance.

The results of the experiments are presented in the Tables 1–6, classified by each approach (presented in Section 3.3) and by diversity Index (presented in Section 2). The approaches tested were:

- RING: decomposition into rings
- RING DIV: decomposition into rings and division of the population into subgroups
- CIRC: decomposition in circles
- CIRC DIV: decomposition in circles and division of the population into subgroups
- VHD: rectangular decomposition
- VHD DIV: decomposing rectangular division of the population into subgroups

The statistics monitored for each experiment were: Sensitivity (S), Specificity (Sp), accuracy (Acc) and Number of Support Vector (nSv). They all are demonstrated by the average results of three runs jointly with the standard deviation.

Since the methodology aims to reduce false positives, we must reach higher rates of sensitivity. This means that there are a smaller number of true positives that are not being detected. Having the highest sensitivity, the second sorting criterion is specificity, that is the rate of false positives reduction.

The RING approach (Table 1) achieved the best sensitivity result of 98.7% when using McIntosh as a descriptor with the ratio 50/50. The RING DIV approach (Table 2) achieved as best result sensitivity of 98.8% using index Camargo in proportion 50/50. Results in both the specificity is 100% and both have a low value nSv.

The CIRC approach (Table 3) obtained the best result sensitivity of 98.7% using the Shannon index in proportion 50/50. The division of the population (Table 4), as happened in the RING approach, led to a slight improvement in the best sensitivity reaching 98.8% using the Camargo index with the proportion 60/40.

The VHD approach (Table 5) achieved as best result a sensitivity of 100% using the Shannon index in proportion 50/50, followed by 99.6% achieved by the indexes J and McIntosh, both in the proportion 50/50. The division population (Table 6), unlike what happened in the previous analysis, reached 99.6 % sensitivity with the Camargo index and 50/50 proportion.

The VHD approach (Table 5) using the Shannon index shows the best overall performance in terms of accuracy, corresponding to 100%. The second best result was also found using the approach VHD followed by Camargo index with the representation of population subgroups (Table 6). The latter reaches 99.9% accuracy, with sensitivity and specificity equal to 99.6 and 99.9% respectively. Important to note that these two best results were found with the 50/50 proportion and used a low number of support vectors, 159 and 108, respectively. The significance of these findings is that these combinations besides being the best result, have also classification models that do not suffer from overfit.

These two best results belong to the approaches that stand with the best results on average, VHD and VHD DIV. These indexes showed poor results in other approaches as Buzas-Gibson and Simpson, obtained performance improvements. The results shows that the spatial division into rectangular regions generate a better division of population groups and pattern. Giving to diversity index, a greater capacity to better represent the groups.

However, this analysis can not be taken as fully conclusive since very similar results were found with other approaches. But this assumption can lead to the discussion is really only important to analyze aspects of circular regions of masses to discriminate then over non-mass regions.

The basic assumption is that non-mass regions tend to have a more random distribution than a mass region that is expected to have homogeneous distribution concentrated in the center and also different forms including spiculated and can also be occluded by regions of the breast parenchyma. We can assume than that corner areas are equally important to discriminate a mass of a non-mass region. Thus, approaches VHD encompassing these regions of the window, can capture these populations which are in turn represented by the diversity indexes, and contribute to aspects of wealth and dominance of texture.

We can still analyze that the approaches of population division generated better results for some indexes and worse for others. Among the indexes that have been highlighted are Camargo, Buzas-Gibson, Total Diversity, Hill and Simpson, mostly evenness

Table 1
Results for RING approach using diversity indexes.

Index	Prop.	Acc	S	Sp	nSV
Berger Parker	50/50	99.6 ± 0.3	98.5 ± 0.0	100.0 ± 0.4	29 ± 14
	60/40	99.6 ± 0.4	98.3 ± 0.0	100.0 ± 0.5	45 ± 10
Brillouin	50/50	99.0 ± 0.1	97.5 ± 0.8	99.5 ± 0.3	74 ± 18
	60/40	99.2 ± 0.2	97.7 ± 0.4	99.7 ± 0.1	86 ± 18
Buzas Gibson	50/50	75.5 ± 0.5	52.7 ± 9.1	83.1 ± 9.4	499 ± 257
	60/40	77.7 ± 0.3	77.7 ± 0.5	77.6 ± 0.1	363 ± 6
Camargo	50/50	94.4 ± 0.3	93.3 ± 1.9	94.7 ± 0.5	107 ± 11
	60/40	93.6 ± 1.1	95.0 ± 2.9	93.1 ± 0.8	163 ± 48
D	50/50	96.3 ± 0.5	91.0 ± 3.4	98.1 ± 0.7	88 ± 12
	60/40	97.4 ± 0.5	94.6 ± 2.4	98.4 ± 0.4	131 ± 45
Diversidade Total	50/50	85.9 ± 1.3	78.5 ± 3.1	88.4 ± 0.9	245 ± 37
	60/40	86.3 ± 2.0	69.8 ± 4.7	91.8 ± 1.0	244 ± 34
Hill	50/50	80.6 ± 1.3	67.3 ± 2.0	85.0 ± 1.8	265 ± 7
	60/40	83.2 ± 1.1	66.7 ± 2.6	88.8 ± 0.7	289 ± 8
J	50/50	99.0 ± 0.1	96.0 ± 0.0	100.0 ± 0.2	89 ± 22
	60/40	99.3 ± 0.1	97.3 ± 0.4	99.9 ± 0.2	104 ± 18
Mcintosh	50/50	99.7 ± 0.2	98.7 ± 0.0	100.0 ± 0.3	52 ± 14
	60/40	99.1 ± 0.5	96.3 ± 0.0	100.0 ± 0.7	49 ± 13
Shannon	50/50	99.6 ± 0.2	98.5 ± 0.0	100.0 ± 0.3	23 ± 5
	60/40	99.4 ± 0.5	97.9 ± 0.4	99.9 ± 0.5	21 ± 4
Simpson	50/50	80.4 ± 0.7	69.3 ± 1.3	84.1 ± 1.1	337 ± 96
	60/40	80.6 ± 0.3	62.7 ± 0.1	86.6 ± 1.0	388 ± 62

Table 2
Results for RING DIV approach using diversity indexes.

Index	Prop.	Acc	S	Sp	nSV
Berger Parker	50/50	99.0 ± 0.3	96.5 ± 0.0	99.8 ± 0.3	110 ± 34
	60/40	99.1 ± 0.1	98.1 ± 1.5	99.4 ± 0.5	50 ± 6
Brillouin	50/50	98.5 ± 0.1	95.5 ± 0.8	99.6 ± 0.2	132 ± 35
	60/40	98.3 ± 1.0	95.0 ± 0.7	99.4 ± 1.1	77 ± 22
Buzas Gibson	50/50	77.4 ± 0.5	25.7 ± 1.5	94.6 ± 1.0	636 ± 68
	60/40	77.3 ± 1.0	22.9 ± 2.9	95.4 ± 1.4	823 ± 74
Camargo	50/50	99.7 ± 0.1	98.8 ± 0.0	100.0 ± 0.1	82 ± 27
	60/40	99.7 ± 0.3	98.8 ± 0.0	100.0 ± 0.4	144 ± 93
D	50/50	90.1 ± 0.3	75.7 ± 0.6	94.9 ± 0.6	268 ± 9
	60/40	92.4 ± 0.8	83.5 ± 1.7	95.4 ± 0.5	302 ± 10
Diversidade Total	50/50	91.6 ± 0.9	83.2 ± 5.5	94.4 ± 1.0	151 ± 34
	60/40	92.1 ± 0.7	83.1 ± 1.2	95.1 ± 0.7	179 ± 42
Hill	50/50	88.5 ± 1.2	73.7 ± 4.0	93.4 ± 0.3	250 ± 79
	60/40	88.7 ± 2.1	71.7 ± 2.6	94.4 ± 3.4	369 ± 3
J	50/50	98.4 ± 0.2	94.8 ± 0.8	99.6 ± 0.4	90 ± 4
	60/40	98.2 ± 0.1	94.2 ± 1.1	99.6 ± 0.3	94 ± 30
Mcintosh	50/50	98.9 ± 0.2	96.8 ± 1.1	99.6 ± 0.2	105 ± 53
	60/40	99.3 ± 0.1	97.3 ± 0.0	100.0 ± 0.1	83 ± 24
Shannon	50/50	98.9 ± 0.0	96.5 ± 0.0	99.7 ± 0.0	111 ± 45
	60/40	99.0 ± 0.6	96.0 ± 0.0	100.0 ± 0.8	131 ± 23
Simpson	50/50	90.3 ± 1.2	76.5 ± 0.8	94.9 ± 1.5	200 ± 31
	60/40	91.8 ± 0.6	82.3 ± 2.4	95.0 ± 1.4	256 ± 9

Table 3
Results for CIRC approach using diversity indexes.

Index	Prop.	Acc	S	Sp	nSV
Berger Parker	50/50	99.6 ± 0.2	98.5 ± 0.3	99.9 ± 0.3	58 ± 24
	60/40	99.4 ± 0.3	97.5 ± 0.0	100.0 ± 0.4	77 ± 22
Brillouin	50/50	96.9 ± 0.9	92.8 ± 1.0	98.2 ± 1.5	140 ± 25
	60/40	96.9 ± 0.3	92.3 ± 0.3	98.5 ± 0.5	150 ± 14
Buzas Gibson	50/50	76.5 ± 1.0	16.5 ± 7.6	96.6 ± 0.9	724 ± 51
	60/40	76.5 ± 0.3	11.0 ± 2.5	98.3 ± 0.3	955 ± 8
Camargo	50/50	91.8 ± 1.0	83.7 ± 2.5	94.4 ± 2.6	300 ± 208
	60/40	93.2 ± 1.8	89.5 ± 5.0	94.6 ± 0.7	191 ± 30
D	50/50	93.3 ± 0.3	86.9 ± 0.6	95.5 ± 0.6	160 ± 39
	60/40	93.6 ± 1.3	86.6 ± 1.9	95.8 ± 1.2	155 ± 8
Diversidade Total	50/50	86.3 ± 1.1	83.5 ± 2.2	87.2 ± 3.4	377 ± 105
	60/40	85.6 ± 1.6	75.0 ± 2.3	88.9 ± 1.6	339 ± 75
Hill	50/50	80.0 ± 0.4	75.9 ± 0.3	81.4 ± 1.5	359 ± 60
	60/40	85.6 ± 9.1	79.6 ± 18.2	88.7 ± 5.1	297 ± 185
J	50/50	96.8 ± 0.8	93.0 ± 2.4	98.2 ± 0.6	115 ± 18
	60/40	97.8 ± 1.0	96.0 ± 3.7	98.5 ± 0.1	116 ± 64
Mcintosh	50/50	99.2 ± 0.0	97.3 ± 0.3	99.9 ± 0.1	44 ± 1
	60/40	99.5 ± 0.1	98.1 ± 0.4	99.9 ± 0.0	64 ± 47
Shannon	50/50	99.7 ± 0.1	98.7 ± 0.0	100.0 ± 0.1	39 ± 16
	60/40	90.9 ± 15.1	63.5 ± 37.1	98.3 ± 13.8	296 ± 423
Simpson	50/50	75.5 ± 0.9	40.5 ± 1.4	87.0 ± 7.0	559 ± 230
	60/40	82.5 ± 14.7	39.8 ± 36.0	98.5 ± 13.9	678 ± 470

indexes. The observation verifies that evenness indexes are highlighted to be analyzed by breaking down its contributions and individual analysis.

In general, for all the approaches, the index that generated the best results on average was the Berger-Parker. His goal is to measure the importance in terms of dominance of the most abundant species in relation to other species. Therefore, based on the results we conclude that the dominant aspect operates in a manner different between the groupings. Analyzing the individuals who represent the masses, we find that their species are concentrated in the upper pixels values. Even after the logarithmic enhancement process. Non-mass individuals, have focus groups scattered between medium and high tones. Although the visual appearance is similar, and perhaps the difference could not be easily seen, the Berger Parker index shows that mass species are spatially concentrated in a small group of high dominance.

4.1. Comparison with other works

Table 7 presents a comparison with another works. To better understand, the comparison is done in terms of features used to describe, machine learning technique, mammography image database and the results of overall accuracy (Acc), area under roc curve (Az), false positive reduction (FPR) and sensibility (S).

All compared studies uses publicly available image databases. Most of all uses SVM as classifier, or ensembles techniques over SVM to better select the training database and avoid randomness. The features extracted for all works have approaches to enhance the description and the performance even for the works that use shape descriptors.

In comparison with other works presented in comparison table, we find an equivalent performance in general. The database is used in regions of greatest use, while the DDSM is known for heteroge-

Table 4
Results for CIRC DIV approach using diversity indexes.

Index	Prop.	Acc	S	Sp	nSV
Berger Parker	50/50	98.0 ± 0.9	94.0 ± 1.3	99.4 ± 0.8	75 ± 14
	60/40	98.5 ± 0.5	96.0 ± 1.3	99.3 ± 0.3	107 ± 39
Brillouin	50/50	97.5 ± 0.2	94.3 ± 0.4	98.5 ± 0.3	104 ± 27
	60/40	97.3 ± 0.4	94.8 ± 1.1	98.1 ± 0.5	109 ± 17
Buzas Gibson	50/50	77.8 ± 0.9	24.8 ± 1.7	95.4 ± 1.7	701 ± 47
	60/40	76.4 ± 0.6	19.6 ± 3.6	95.3 ± 0.5	849 ± 16
Camargo	50/50	99.5 ± 0.3	98.5 ± 0.3	99.9 ± 0.3	74 ± 55
	60/40	99.6 ± 0.1	98.8 ± 0.4	99.9 ± 0.2	61 ± 23
D	50/50	83.8 ± 0.4	71.5 ± 0.5	87.9 ± 0.8	281 ± 17
	60/40	85.8 ± 1.5	72.9 ± 2.8	90.1 ± 1.3	307 ± 6
Diversidade Total	50/50	89.0 ± 0.4	79.5 ± 3.7	92.1 ± 1.2	163 ± 9
	60/40	90.3 ± 2.1	80.6 ± 2.4	93.5 ± 2.4	191 ± 12
Hill	50/50	88.9 ± 1.1	80.7 ± 1.6	91.6 ± 1.1	341 ± 58
	60/40	88.6 ± 0.6	74.4 ± 3.6	93.3 ± 1.3	318 ± 57
J	50/50	96.8 ± 0.8	89.5 ± 1.4	99.2 ± 0.9	226 ± 87
	60/40	96.9 ± 0.6	93.1 ± 1.5	98.2 ± 0.5	174 ± 114
Mcintosh	50/50	97.7 ± 0.2	95.0 ± 0.7	98.6 ± 0.0	79 ± 15
	60/40	97.6 ± 0.2	94.6 ± 0.9	98.6 ± 0.1	143 ± 70
Shannon	50/50	97.7 ± 0.4	94.2 ± 0.9	98.8 ± 0.3	134 ± 50
	60/40	97.5 ± 0.7	95.0 ± 1.1	98.3 ± 0.7	160 ± 42
Simpson	50/50	88.9 ± 0.4	72.7 ± 1.4	94.3 ± 0.3	191 ± 32
	60/40	89.8 ± 1.4	76.9 ± 1.8	94.2 ± 1.8	240 ± 8

Table 5
Results for VHD approach using diversity indexes.

Index	Prop.	Acc	S	Sp	nSV
Berger Parker	50/50	99.8 ± 0.3	98.9 ± 0.0	100.0 ± 0.4	168 ± 123
	60/40	99.5 ± 0.3	98.3 ± 0.3	99.9 ± 0.3	158 ± 166
Brillouin	50/50	99.3 ± 0.1	97.3 ± 0.3	99.9 ± 0.1	128 ± 99
	60/40	96.2 ± 6.1	94.0 ± 14.4	96.2 ± 2.8	205 ± 148
Buzas Gibson	50/50	90.0 ± 2.4	84.8 ± 5.4	91.6 ± 2.0	318 ± 123
	60/40	92.8 ± 5.5	85.8 ± 11.1	95.8 ± 4.3	252 ± 186
Camargo	50/50	99.6 ± 0.1	99.5 ± 0.5	99.6 ± 0.2	102 ± 48
	60/40	97.2 ± 4.5	91.5 ± 6.9	98.5 ± 3.8	157 ± 70
D	50/50	92.0 ± 0.2	78.4 ± 0.1	96.5 ± 0.3	280 ± 118
	60/40	94.2 ± 3.7	86.3 ± 6.5	97.2 ± 3.1	249 ± 152
Diversidade Total	50/50	97.8 ± 0.9	93.4 ± 0.6	99.2 ± 1.0	142 ± 27
	60/40	89.7 ± 12.6	56.2 ± 2.8	99.4 ± 12.7	351 ± 392
Hill	50/50	74.4 ± 1.0	18.4 ± 34.2	93.0 ± 4.6	699 ± 322
	60/40	83.3 ± 14.2	38.5 ± 28.7	99.9 ± 14.2	660 ± 519
J	50/50	99.8 ± 0.1	99.6 ± 0.1	99.8 ± 0.1	149 ± 96
	60/40	99.6 ± 0.5	99.2 ± 1.4	99.7 ± 0.1	134 ± 60
Mcintosh	50/50	99.9 ± 0.1	99.6 ± 0.3	99.9 ± 0.1	66 ± 26
	60/40	99.8 ± 0.1	99.2 ± 0.0	100.0 ± 0.1	213 ± 56
Shannon	50/50	100.0 ± 0.0	100.0 ± 0.0	100.0 ± 0.0	159 ± 69
	60/40	91.6 ± 14.5	61.9 ± 34.6	99.8 ± 14.4	403 ± 343
Simpson	50/50	74.9 ± 0.3	0.4 ± 0.0	99.8 ± 0.1	853 ± 92
	60/40	50.1 ± 43.4	0.6 ± 57.7	100.0 ± 43.4	640 ± 554

neous structures. Although it is not possible to compare the generality of the classifiers created by each compared work, since it does not show information to indicate that information, we can affirm that for the database used, this methodology proved robust and generic classification of ROI's into the class mass and non-mass, and promote the reduction of false positives.

5. Conclusions

This paper presented a research on the application of diversity indexes and spatial approaches for the reduction of false positives in mass detection methodologies under digitized mammography's regions. It has been shown that these indexes can quantify with the aid of spatial approaches, texture characteristics able to differentiate masses and non-mass ROI's.

To use the concept of Diversity Analysis, some mappings concepts took the deduction of a species could be represented by an intensity present in the region of analysis. Thus, the proposed methodology presented results based on analysis of the behavior of these species over spatially sampled regions.

For the field of pattern recognition, we conclude that the use of diversity indexes with spatial decomposition approaches, generate a description highly discriminant when it is applied for distinction of masses and non-masses regions. Even if we consider the simplicity of diversity index, represented by the concepts of evenness, dominance and diversity.

The proposed methodology submits the generated characteristic vectors for classification with unbalanced database, prioritizing sensitivity. Even in that situation, obtained promising results to reduce false positives, represented by rates of specificity while sensitivity curve remained high.

The presented experiments lead us to examine assumptions as the importance of boundary regions present in the masses for their discrimination. The mass is a circle region-based, or spiculated, but with convex c. We present the results of this work through a mechanism of extracting texture can realize local changes and absorb

Table 6
Results for VHD DIV approach using diversity indexes.

Index	Prop.	Acc	S	Sp	nSV
Berger Parker	50/50	99.7 ± 0.1	99.1 ± 0.3	99.9 ± 0.2	191 ± 70
	60/40	99.2 ± 0.2	97.1 ± 0.6	99.9 ± 0.1	140 ± 13
Brillouin	50/50	99.0 ± 0.4	97.3 ± 1.4	99.5 ± 0.2	246 ± 41
	60/40	94.0 ± 8.9	82.1 ± 14.7	96.9 ± 7.6	304 ± 117
Buzas Gibson	50/50	82.2 ± 1.0	52.7 ± 4.9	92.0 ± 3.8	530 ± 203
	60/40	90.1 ± 8.6	75.4 ± 14.4	96.0 ± 7.3	252 ± 151
Camargo	50/50	99.9 ± 0.1	99.6 ± 0.3	99.9 ± 0.2	108 ± 32
	60/40	94.1 ± 10.2	82.3 ± 18.3	96.8 ± 8.3	217 ± 171
D	50/50	81.7 ± 2.8	43.7 ± 5.7	94.0 ± 4.4	525 ± 198
	60/40	86.2 ± 4.6	66.3 ± 7.9	93.4 ± 5.0	512 ± 202
Diversidade Total	50/50	90.2 ± 2.0	74.8 ± 3.0	95.1 ± 1.9	390 ± 20
	60/40	86.1 ± 9.3	47.7 ± 7.2	97.8 ± 10.1	569 ± 217
Hill	50/50	81.6 ± 0.9	52.0 ± 2.9	91.4 ± 1.9	520 ± 36
	60/40	86.6 ± 10.7	63.8 ± 18.4	95.4 ± 9.5	540 ± 353
J	50/50	98.9 ± 0.5	95.9 ± 0.3	99.9 ± 0.8	174 ± 47
	60/40	98.9 ± 0.5	95.6 ± 0.3	99.9 ± 0.6	137 ± 53
Mcintosh	50/50	99.4 ± 0.1	97.7 ± 0.0	100.0 ± 0.1	105 ± 7
	60/40	99.3 ± 0.4	97.3 ± 0.0	100.0 ± 0.5	136 ± 22
Shannon	50/50	99.0 ± 0.2	96.4 ± 0.9	99.8 ± 0.1	161 ± 38
	60/40	91.8 ± 13.4	62.7 ± 8.2	99.9 ± 13.5	399 ± 344
Simpson	50/50	83.6 ± 0.8	49.3 ± 2.4	95.0 ± 0.5	553 ± 46
	60/40	88.5 ± 9.7	67.1 ± 14.7	96.8 ± 8.8	430 ± 300

Table 7
Summary of comparison works, organized by year of publication, where (M/N) means the number of masses and non-mass regions, Az area under the ROC curve, the overall accuracy Acc, FPR the false positive reduction rate and S, sensibility.

Works	Year	Features Used	Machine Learning	Database (M/N)	Results
(Lladó et al., 2009)	2009	Texture - LBP	SVM	DDSM - 1792(256/1536)	Az = 0.94
(Braz Junior et al., 2009)	2009	Geostatistical - Directional	SVM	DDSM - 1394(584/810)	Az = 1.00
(Masotti et al., 2009)	2009	Ranklet Transformation	SVM	DDSM - 1501(251/1250)	S = 80%, FPR = 35%
(Moayedi et al., 2010)	2010	Counterlet Coefficients, Co-Occurrence and Morphology	SELwSVM	MIAS - 90 (30/90)	Acc = 0.966
(Eltoukhy et al., 2010b)	2010	Wavelet + Counterlet	Nearest Neighbor Classifier	–	Acc = 0.95
(Muralidhar et al., 2010)	2010	SnakeRules + Shape Features	Especilist System	312(36/276)	Az = 0.79
(Carvalho et al., 2012)	2012	Diversity + (GLRLM + GLCM)	SVM	DDSM - 800(400/400)	Acc = 0.99
(Surendiran & Vadivel, 2012)	2012	Shape Features	CART	1552(939/613)	Acc = 0.95
(Hussain et al., 2012)	2012	Gabor Features	SELwSVM	MIAS - 99(55/54)	Az = 1.0
Our Work	–	Spatial diversity analysis	SVM	DDSM - 1600(400/1200)	Best Acc = 100%, Best FPR = 100%

them through diversity indexes. These changes together may be contributed to describe the overall texture of masses also geometrically since the decomposition space is a way to preserve local relations at the same time they are described.

Local texture analysis measures changes in small situations and could be extracted by the spatial approach used and configures as an important conclusion from this study. Also as a starting point for further work. Diversity analysis measures essentially global features about certain population. The division of species into subpopulations resulted a gain of performance for certain index. So, the way of the species are extracted, organized and analyzed, directly influences the result obtained by the index.

As future work we propose to initially test with other databases in generated by detection methodologies. We intend to use an extension of diversity measures to adapt to local conditions, especially the capture of patterns present intra mass regions and promote the diagnosis of masses according to their nature of malignancy. With this, complete the classification methodology with diagnosis of lesions, which is a key step for mammogram interpretation,

Acknowledgment

The authors would acknowledge CAPES, FAPEMA and CNPq for the financial support.

References

(ACS), A.C.S. (2011). Learn about breast cancer. <http://www.cancer.org>.

Altman, D., & Bland, J. (1994). Diagnostic tests 1: Sensitivity and specificity.. *BMJ: British Medical Journal, 308*, 1552–1562.

Sampaio, W. Borges, Diniz, E. Moraes, Silva, A. CorrOa, Paiva, A. Cardoso de, & Gattass, M. (2011). Detection of masses in mammogram images using CNN, geostatistic functions and SVM. *Computers in Biology and Medicine, 41*, 653–664.

Bozek, J., Mustra, M., Delac, K., & Grgic, M. (2009). A survey of image processing algorithms in digital mammography. Recent advances in multimedia signal processing and communications, (pp. 631–657).

Braz Junior, G., Paiva, A. Cardoso de, Silva, A. Corrêa, & Oliveira, A. Cesar Muniz de (2009). Classification of breast tissues using moran's index and geary's coefficient as texture signatures and svm. *Computers in Biology and Medicine, 39*, 1063–1072.

Braz Junior, G., Rocha, S. V., Silva, A. C., & Paiva, A. C. (2013). A false positive reduction in mass detection approach using spatial diversity analysis. In *The fifth international conference on ehealth, telemedicine and social medicine* (pp. 208–213).

Burhenne, L. J. W., Wood, S. A., D'Orsi, C. J., Feig, S. A., Kopans, D. B., O'Shaughnessy, K. F., Sickles, E. A., Tabar, L., Vyborny, C. J., & Castellino, R. A. (2000). *1. Radiology, 215*, 554–562.

Buzas, M., & Hayek, L. (1998). She analysis for biofacies identification. *The Journal of Foraminiferal Research, 28*, 233–239.

Camargo, J. (1993). Must dominance increase with the number of subordinate species in competitive interactions. *Journal of Theoretical Biology, 161*, 537–542.

Carvalho, P. M. d. S., Paiva, A. C., & Silva, A. C. (2012). Classification of breast tissues in mammographic images in mass and non-mass using mcintosh's diversity index and svm. In *MLDM'12 Proceedings of the 8th international conference on machine learning and data mining in pattern recognition* (pp. 482–494). ACM.

Cheikhrouhou, I., Djemal, K., & Maaref, H. (2011). Protuberance selection descriptor for breast cancer diagnosis. In *(EUVIP), 2011 3rd European workshop on visual information processing* (pp. 280–285). Institute of Electrical and Electronics Engineers (IEEE).

Cheng, H., Shi, X., Min, R., Hu, L., Cai, X., & Du, H. (2006). Approaches for automated detection and classification of masses in mammograms. *Pattern Recognition, 39*, 646–668.

Dean, J. C., & Ilvento, C. C. (2006). Improved cancer detection using computer-aided detection with diagnostic and screening mammography: prospective study of 104 cancers. *American Journal of Roentgenology, 187*, 20–28.

Elter, M., & Horsch, A. (2009). CADx of mammographic masses and clustered microcalcifications: A review. *Medical Physics, 36*, 2052–2068.

Eltoukhy, M. M., Faye, I., & Samir, B. B. (2010a). Breast cancer diagnosis in digital mammogram using multiscale curvelet transform. *Computerized Medical Imaging and Graphics, 4* (296–276).

Eltoukhy, M. M., Faye, I., & Samir, B. B. (2010b). A comparison of wavelet and curvelet for breast cancer diagnosis in digital mammogram. *Computers in Biology and Medicine, 40*, 384–391.

Fenton, J. J., Taplin, S. H., Carney, P. A., Abraham, L., Sickles, E. A., D'Orsi, C., et al. (2007). Influence of computer-aided detection on performance of screening mammography. *New England Journal of Medicine, 356*, 1399–1409 (PMID: 17409321).

Freer, T. W., & Ulissey, M. J. (2001). *1. Radiology, 220*, 781–786.

Heath, M., Bowyer, K., & Kopans, D. (1998). Current status of the digital database for screening mammography. In *Digital mammography* (pp. 457–460). Kluwer Academic Publishers.

Hill, M. O. (1973). Diversity and evenness: A unifying notation and its consequences. *Ecology, 54*, 427–432.

Houssami, N., Ciatto, S., Irwig, L., Simpson, J., & Macaskill, P. (2002). The comparative sensitivity of mammography and ultrasound in women with breast symptoms: An age-specific analysis. *The Breast, 11*, 125–130.

Hussain, M., Khan, S., Muhammad, G., & Bebis, G. (2012). A comparison of different gabor features for mass classification in mammography. In *2012 Eighth international conference on signal image technology and internet based systems (SITIS)* (pp. 142–148).

Jost, L. (2010). The relation between evenness and diversity. *Diversity, 2*, 207–232.

Karssemeijer, N., Frieling, J., & Hendriks, J. (1993). Spatial resolution in digital mammography. *Investigative Radiology, 28*, 413.

Ko, J. M., Nicholas, M. J., Mendel, J. B., & Slanetz, P. J. (2006). Prospective assessment of computer-aided detection in interpretation of screening mammography. *American Journal of Roentgenology, 187*, 1483–1491.

Liu, X., Liu, J., Zhou, D., & Tang, J. (2010). A benign and malignant mass classification algorithm based on an improved level set segmentation and texture feature analysis. In *2010 4th International conference on bioinformatics and biomedical engineering (iCBBE)* (pp. 1–4). IEEE.

Lladó, X., Oliver, A., Freixenet, J., Martí, R., & Martí, J. (2009). A textural approach for mass false positive reduction in mammography. *Computerized Medical Imaging and Graphics, 33*, 415–422.

Magurran, A. (2004). *Measuring biological diversity*. Taylor & Francis.

Magurran, A. (1988). *Ecological diversity and its measurement* (vol. 179). NJ: Princeton university press Princeton.

Masotti, M., Lanconelli, N., & Campanini, R. (2009). Computer-aided mass detection in mammography: False positive reduction via gray-scale invariant ranklet texture features. *Medical Physics, 36*, 311–316.

May, R. (1975). Patterns of species abundance and diversity. *Ecology and evolution of communities*, 81–120.

Moayedi, F., Azimifar, Z., Boostani, R., & Katebi, S. (2010). Contourlet-based mammography mass classification using the svm family. *Computers in Biology and Medicine, 40*, 373–383.

Muralidhar, G., Markey, M., & Bovik, A. (2010). Snakules for automatic classification of candidate spiculated mass locations on mammography. In *2010 IEEE southwest symposium on image analysis interpretation (SSIAI)* (pp. 197–200).

Nanni, L., Lumini, A., & Brahnam, S. (2012). Survey on LBP based texture descriptors for image classification. *Expert Systems with Applications, 39*, 3634–3641.

Nunes, A. P., Silva, A. C., & Paiva, A. C. D. (2010). Detection of masses in mammographic images using geometry, simpson's diversity index and SVM. *International Journal of Signal and Imaging Systems Engineering, 3*, 40–51.

Pielou, E. (1975). *Ecological diversity*. New York: Wiley.

Rangayyan, R. M., Ayres, F. J., & Desautels, J. Leo (2007). A review of computer-aided diagnosis of breast cancer: Toward the detection of subtle signs. *Journal of the Franklin Institute, 344*, 312–348.

Shannon, C. (2001). A mathematical theory of communication. *ACM SIGMOBILE Mobile Computing and Communications Review, 5*, 3–55.

Shi, J., Sahiner, B., Chan, H., Ge, J., Hadjiiski, L., Helvie, M., et al. (2008). Characterization of mammographic masses based on level set segmentation with new image features and patient information. *Medical Physics, 35*, 280.

Simpson, E. (1994). Measurement of diversity. *Nature*.

Carvalho, P. M. de Sousa, Paiva, A. C. de, & Silva, A. C. (2012). Classification of breast tissues in m ammographic images in m ass and non-mass using mcintosh's diversity index and SVM. In *Proceedings of the 8th international conference on machine learning and data mining in pattern recognition MLDM'12* (pp. 482–494). Berlin, Heidelberg: Springer-Verlag.

Surendiran, B., & Vadivel, A. (2010). Feature selection using stepwise anova, discriminant analysis for mammogram mass classification. *International Journal on Recent Trends in Engineering, 3*, 55–57.

Surendiran, B., & Vadivel, A. (2012). Mammogram mass classification using various geometric shape and margin features for early detection of breast cancer. *International Journal of Medical Engineering and Informatics, 4*, 36–54.

Tang, J., Rangayyan, R., Xu, J., El Naqa, I., & Yang, Y. (2009). Computer-aided detection and diagnosis of breast cancer with mammography: Recent advances. *IEEE Transactions on Information Technology in Biomedicine, 13*, 236–251.

Tralic, D., Bozek, J., & Grgic, S. (2011). Shape analysis and classification of masses in mammographic images using neural networks. In *2011 18th International conference on systems, signals and image processing (IWSSIP)* (pp. 1–5). IEEE.

Vapnik, V. (2000). *The nature of statistical learning theory*. Springer Verlag.

Varela, C., Timp, S., & Karssemeijer, N. (2006). Use of border information in the classification of mammographic masses. *Physics in Medicine and Biology, 51*, 425–442.

Verma, B. (2008). Novel network architecture and learning algorithm for the classification of mass abnormalities in digitized mammograms. *Artificial Intelligence in Medicine, 42*, 67–79.